

## Preparation and Adsorption Properties of Diethylenetriamine-Modified Chitosan Beads for Acid Dyes

Yikai Yan, Bo Xiang, Yijiu Li, Qian Jia

Department of Chemistry, Tongji University, Shanghai 200092, China

Correspondence to: B. Xiang (E-mail: bxiangbo@tongji.edu.cn)

**ABSTRACT:** This work has demonstrated that the novel chitosan derivative, synthesized by phase transition and grafting diethylenetriamine, has a great potential for the adsorption of acid dyes from aqueous solutions. Four acid dyes with different molecular sizes and structures were used to investigate the adsorption performance of diethylenetriamine-modified chitosan beads (CTSN-beads). Results indicated that the adsorption of dyes on CTSN-beads was largely dependent on the pH value and controlled by the electrostatic attraction. In addition, the adsorption rate (AO10 > AO7 > AR18 > AG25) and adsorption capacities (AO7 > AR18 > AO10 > AG25) were directly related to the molecular size of the dye and the amount of the sulfonate groups on the dye molecules. The equilibrium and kinetic data fitted well with the Langmuir–Freundlich and pseudo-second-order model. Furthermore, thermodynamic parameters indicated that the adsorption processes occurred spontaneously and higher temperature made the adsorption easier. The reuse tests indicated that the CTSN-beads can be recovered for multiple uses. © 2013 Wiley Periodicals, Inc. *J. Appl. Polym. Sci.* 130: 4090–4098, 2013

**KEYWORDS:** adsorption; biomaterials; biopolymers and renewable polymers; dyes/pigments

Received 8 November 2012; accepted 19 June 2013; Published online 8 July 2013

DOI: 10.1002/app.39691

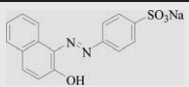
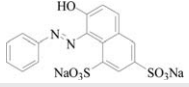
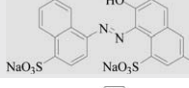
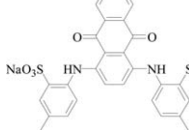
### INTRODUCTION

Most dyes are considered to be toxic and carcinogenic, which are released from the textile, paper, plastics, and dyestuffs industries.<sup>1</sup> Various kinds of acid dyes can be used for dyeing wool, silk, and chinlon. However, it is very difficult to remove these dyes from wastewater since the recalcitrant molecules of dyes (particularly azo dyes) are resistant to aerobic digestion. Nowadays, the treatment of these effluents is a major concern, several techniques have been extensively reported, such as chemical oxidation,<sup>2</sup> electrochemical technique,<sup>3</sup> membrane filtration,<sup>4</sup> adsorption,<sup>5,6</sup> bio-degradation,<sup>7</sup> ozonation,<sup>8</sup> and coagulation.<sup>9</sup> Among these methods of dye removal, adsorption using low-cost adsorbents is an effective and economic method for water decontamination.

Recently, much attention has been focused on various bio-adsorbent materials such as starch,<sup>10</sup> fungal,<sup>11</sup> chitin,<sup>12</sup> and synthetic biopolymers<sup>13</sup> which are environment friendly and can be obtained in large quantity. Chitosan as natural polysaccharide has been developed for high potential of adsorption for dyes; furthermore, it is an abundant, inexpensive, renewable, and fully biodegradable natural raw material. Chitosan is the deacetylated chitin, which is the second most abundant biopolymer in nature. Some studies have showed the chitosan in uptake of various kinds of dyestuffs, such as acid, base, and reactive dyes.<sup>14,15</sup>

Generally, the form of raw chitosan is flake or powder with nonporous and low specific surface area, which limits the dyes to access the interior active adsorption sites. To overcome this obstacle, more attention has been paid to prepare porous chitosan beads. Researchers have found the bead type of chitosan exhibited a greater sorption capacity than that of the flake type.<sup>16,17</sup> On the other hand, several studies have indicated that amino groups in chitosan are the main sites for the adsorption of dyes, and it is an effective way to improve the adsorption ability of chitosan by increasing new active adsorption sites. In this article, porous chitosan bead was chemically modified to get excellent adsorption character for some dyes. And experiments proved that porous structure and functional groups were good for adsorption of dyes. This study includes two steps: the preparation of chitosan beads and the introduction of diethylenetriamine onto chitosan backbone. The chitosan beads were prepared by phase inversion method using sodium hydroxide as bath. The gel formation process can reduce the crystallinity of chitosan. The aim of chitosan modification is to increase the amount and effective percentage of active groups, and enhance the adsorption capacity for acid dyes. The benzaldehyde was firstly chosen to protect the raw amino group in chitosan by Schiff-base reaction. Secondly, the epichlorohydrin was grafted on chitosan beads to provide epoxy group. The diethylenetriamine was further reacted with epoxy to introduce new amino group. At last the products were obtained by removing the

**Table I.** Characteristic and Structure of the Adsorbates Used in This Study

Generic name	Abbreviation	Fw	$\lambda_{\max}$ (nm)	Structure
Acid orange 7	AO7	350.3	485	
Acid orange 10	AO10	452.4	475	
Acid red 18	AR18	604.5	506	
Acid green 25	AG25	622.6	642	

benzaldehyde. The structure of diethylenetriamine-modified chitosan beads (CTSN-beads) was characterized by scanning electric microscopy. FTIR spectra were applied to confirm the change of functional groups. Furthermore, the adsorption behaviors of the CTSN-beads for various dyes were studied to obtain new insights into the intermolecular interaction between dyes and the CTSN-beads.

## EXPERIMENTAL

### Materials and Techniques

Chitosan (91.2% of deacetylation degree) used in this study was purchased from Sinopharm chemical reagent Co. Four commercially available textile dyestuffs were used in this research including three azo dyes (AO7, AO10, and AR18) and one anthraquinone dye (AG25). The chemical structure and characteristics of these dyes are listed in Table I. All dyes and reagents were purchased from Sigma and used without further purification. Fourier transform infrared spectra were recorded on Nicolet FTIR NEXUS spectrometer with KBr pellets in the 4000–500  $\text{cm}^{-1}$  regions. Elemental analysis was determined with the Elementar Vario Cube CN elemental analyzer. Specific surface area was determined by TRISTAE3000 BET determinator and obtained by equation of BET (Brunauer–Emmett–Teller).UV–vis spectra were measured on Agilent-8453 spectrometer.

### Preparation of Chitosan-Beads

The preparation of chitosan-beads (CTS-beads) is described as in previous report.<sup>18</sup> Chitosan solution was prepared by dissolving 4 g chitosan flakes into the 96 g, 4% (m/m) acetic acid solution. The aqueous solution was left to stay still overnight for defoaming after strong stirring. The solution was dropped from the burette into a coagulation bath (sodium hydroxide 2 mol  $\text{L}^{-1}$ ). After stirred for 24 h, the beads kept their initial spherical forms and formed uniform balls (diameter 2.3–2.7 mm). The products were washed thoroughly with deionized water for several times.

### Preparation of Diethylenetriamine-Modified Chitosan Beads

The CTSN-beads were prepared by a modified procedure as referred in the literature.<sup>19,20</sup> The procedure is depicted in

Figure 1. Benzaldehyde (50 g) was slowly added into the mixture of 10 g CTS-beads (water content 96%) and 500 mL deionized water. The benzaldehyde can protect C2 amino group in chitosan from diethylenetriamine. The chitosan-benzaldehyde-beads (CTB-beads) were obtained after the mixture was stirred for 12 h at room temperature. The beads obtained were washed by methanol to remove the unreacted benzaldehyde. Then the intermediate, epoxy chitosan-beads (CTSO-beads) were prepared from 10 g of CTB-beads with 60 mL epichlorohydrin under alkaline condition and 50°C for 8 h. The CTSO-beads further reacted with diethylenetriamine to graft amino groups onto chitosan (CTSSN-beads) at 60°C for 6 h. The acquired CTSSN-beads were dipped into the 2% hydrochloride solution for 48 h to remove the benzaldehyde. The products (CTSN-beads) were washed with distilled water, alcohol, and dilute HCl solution in sequence.

### Adsorption Experiments

The temperature of all experiments was maintained at 25°C, apart from the investigation for the effect of temperature on the sorption, and the batch experiments were agitated for 24 h with a shaking speed of 200 rpm. Anionic dye solution was prepared by dissolving dye in deionized water to the required concentration.

For the influence of pH on the sorption, the mixture of CTSN-beads (0.016 g dry basis of CTSN-beads) and 800 mg  $\text{L}^{-1}$  dye solution (50 mL) were adjusted to a pH range of 3–12. The samples were placed in a series of 100 mL flasks and shaken for 24 h. The residual concentration of the dye was determined spectrophotometrically at  $\lambda_{\max}$  of each dye.

In experiments of batch kinetic adsorption, 800 mg  $\text{L}^{-1}$  dye solution (200 mL) were shaken with adsorbents (0.064 g dry basis of CTSN-beads) in a water bath for predetermined intervals of times. The pH value was controlled at 4, and the concentrations were determined using a UV/visible spectrometry.

The effect of temperature in a range of 25–45°C on the efficiency of adsorbents was carried out in 50 mL of dye solutions (800 mg  $\text{L}^{-1}$ , pH 4). After adding beads, the flasks were

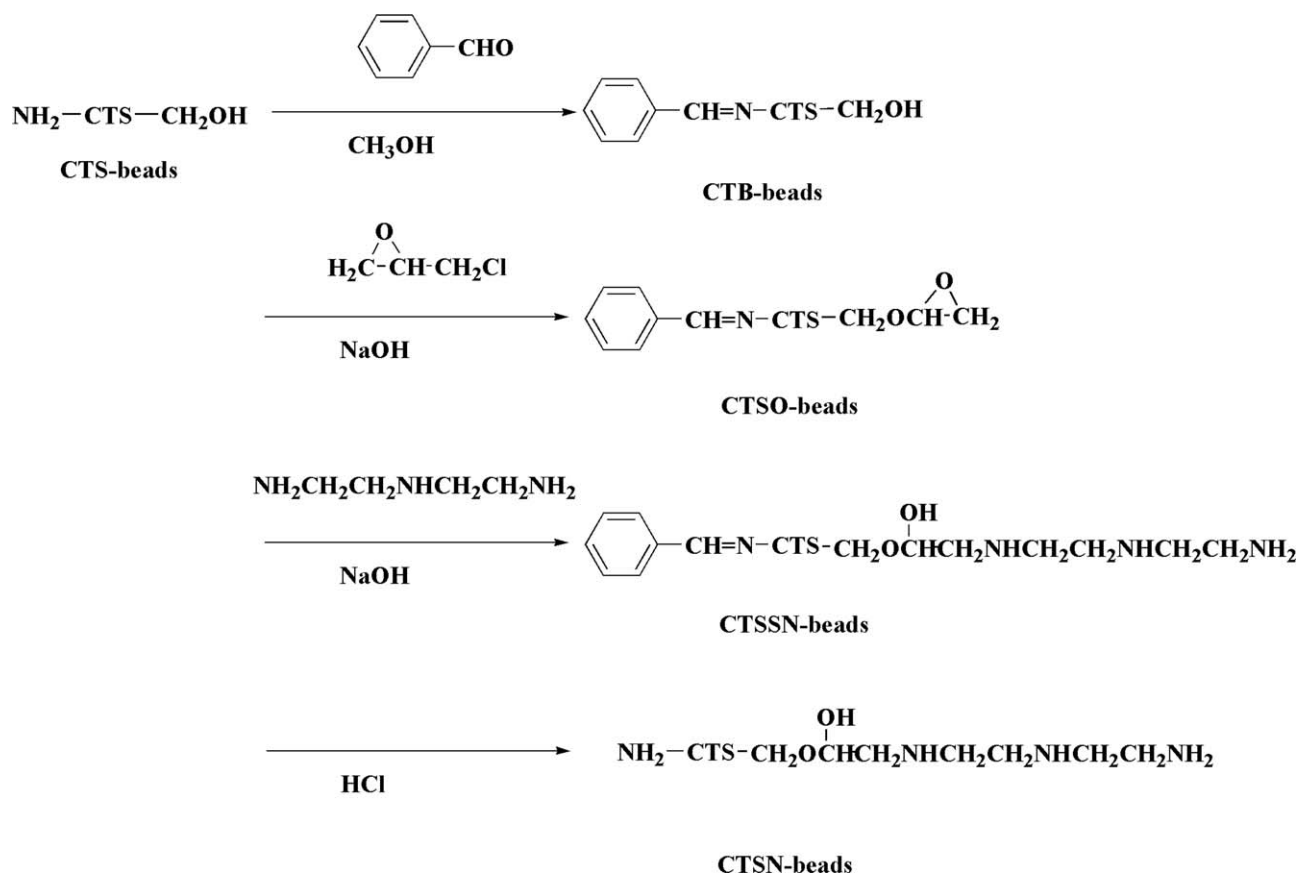


Figure 1. A schematic representation of preparation of CTSN-beads.

agitated in a water bath to maintain the definite temperature. The residual concentrations of dyes were calculated after the volume correction.

For the study of equilibrium sorption, a fixed mass of CTSN-beads (0.016 g dry basis of CTSN-beads) were added into flasks and agitated with dye solutions (varied from 500 mg L<sup>-1</sup> to 1600 mg L<sup>-1</sup>) at pH 4. After filtration, the concentration of each dye solution was determined. Equation (1) was used to calculate the unit mass of CTSN-beads:

$$q_e = \left( \frac{(C_0 - C_e) \times V}{mM} \right) \quad (1)$$

where  $q_e$  is the capacity of absorbent (mmol g<sup>-1</sup>);  $C_0$  and  $C_e$  are the initial and equilibrium solution concentration (mg L<sup>-1</sup>);  $V$  is the volume of solution (L);  $m$  and  $M$  are the dose of absorbent (dry basis, g) and the molecule weight of the dye (g mol<sup>-1</sup>).

For the regeneration test, the CTSN-beads were loaded with dyes using 50 mL of 800 mg L<sup>-1</sup> dyes solution at pH 4. The dyes loaded CTSN-beads were collected and washed with distilled water to remove any unadsorbed dyes, and then were agitated with 50 mL of Na<sub>2</sub>SO<sub>4</sub>/NaOH (pH 12.0) for 6 h. The CTSN-beads after regeneration were reloaded with dyes. This process was repeated for five times to evaluate the reusability of CTSN-beads.

## RESULTS AND DISCUSSION

### Characterization of CTSN-Beads

The surface condition of adsorbents is very important. Figure 2 shows the scanning electron microscope (SEM) images obtained for both materials. It can be seen that the surfaces of the beads have many pores and are uniformly distributed. Such pores are helpful not only for the increase of amine groups but also for the mass transfer of dyes.<sup>21</sup> The surface of the CTSN-beads became rougher due to the multi-step reaction, which could provide more active site for adsorption. The results (Table II) of specific surface area tests also confirmed this conclusion. The drying methods influence the specific surface area significantly. The vacuum-freeze drying was adopted for the BET measurement. The pores and net structure will be destroyed during the normal drying process. The form of raw chitosan is flake or powder which is nonporous and has low specific surface area. However the bead is net structure which is full of water. After drying, the air takes the place of water inside the bead. This process can increase the surface area of beads.

FTIR spectra were also applied to confirm the change of functional group. The difference in FTIR spectra between CTS-beads and its derivatives are shown in Figure 3 in the region of 4000–500 cm<sup>-1</sup>. It was found that CTS-beads and its derivatives all show a broad and strong coupling vibration of –NH<sub>2</sub> and –OH stretching vibrations at 3420 cm<sup>-1</sup>. The major bands for

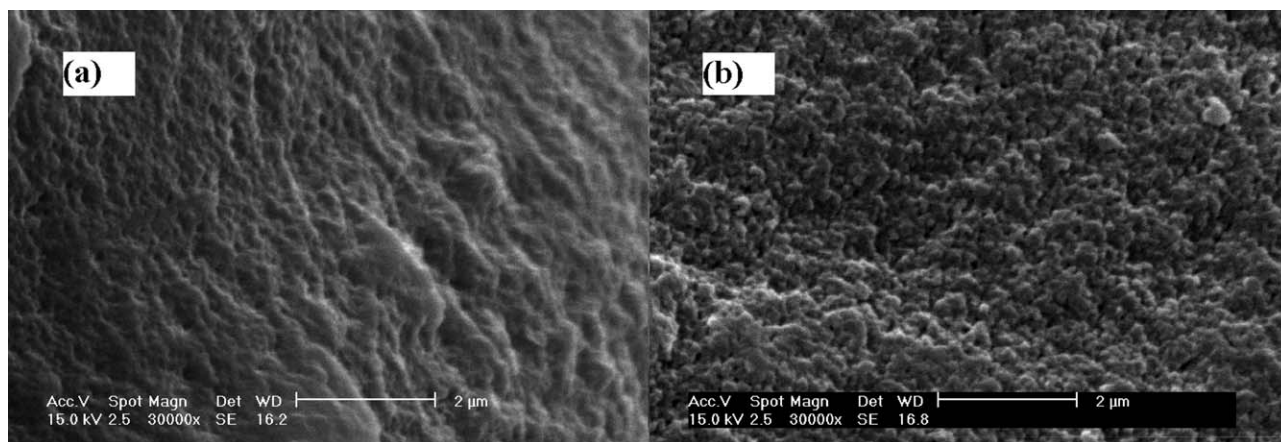


Figure 2. SEM photograph of product: (a) CTS-beads and (b) CTSN-beads.

Table II. Elemental Analysis and Specific Surface Area Analysis Results of CTS and Its Derivatives

Adsorbent	Found (%)			BET surface area (m <sup>2</sup> g <sup>-1</sup> )	Amino groups density (mmol g <sup>-1</sup> )
	C	H	N		
CTS	39.45	6.21	6.38	0.235	3.75
CTS-beads	40.51	6.45	6.21	3.477	3.65
CTSN-beads	44.86	7.63	16.89	5.568	9.94

the CTS-beads can be assigned as follows: 2900 cm<sup>-1</sup> (—C—H stretching vibration in chitosan ring backbone), 1071 cm<sup>-1</sup> (C—O—C stretching vibration in chitosan ring backbone), 1156 cm<sup>-1</sup> (—CN stretching vibration), 1026 cm<sup>-1</sup> (—CO stretching vibration), and 900 cm<sup>-1</sup> (the characteristic peak of β-D-pyranoid ring).<sup>22,23</sup> In the case of CTB-beads, the characteristic peak of benzene ring backbone vibration was clearly observed at 1598 cm<sup>-1</sup>, and the peak of aromatic —CH— out of plane deformation appears at 693 cm<sup>-1</sup> and 754 cm<sup>-1</sup>. These characteristic

peaks also exist in CTSO-beads and CTSSN-beads, and disappear in CTSN-beads because of the removal of benzaldehyde group. It could be confirmed by above arguments that the benzaldehyde group successfully grafted on the backbone of chitosan. CTSN-beads show that a broader and stronger coupling vibration in the region of 3200–3400 cm<sup>-1</sup>, and CTSSN-beads owing to the exposing of amino groups by removing benzaldehyde, and the additional peak appears at 1509 cm<sup>-1</sup> attributed

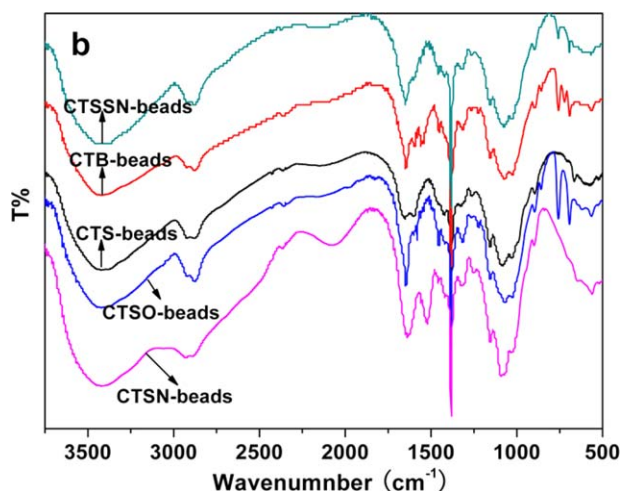


Figure 3. FTIR spectra of CTS-beads and its derivatives. [Color figure can be viewed in the online issue, which is available at wileyonlinelibrary.com.]

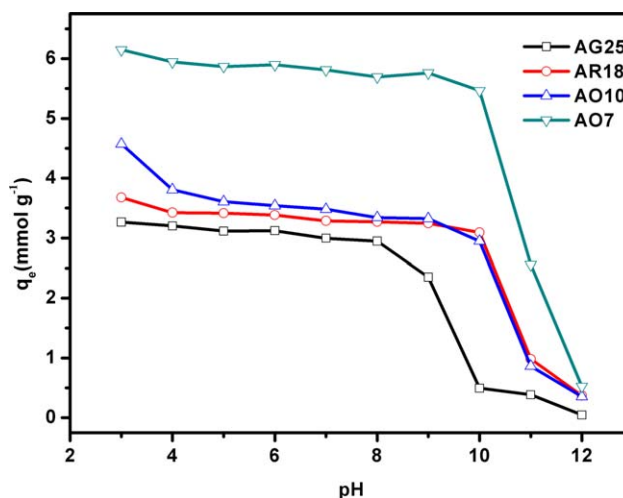


Figure 4. Effect of pH on acid dyes adsorption onto CTSN-beads. [Color figure can be viewed in the online issue, which is available at wileyonlinelibrary.com.]



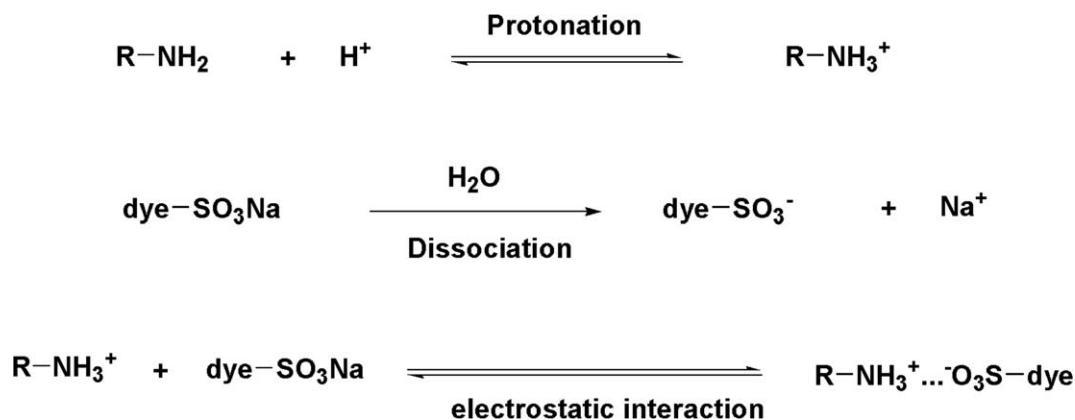


Figure 5. The electrostatic interaction between CTSN-beads and dyes.

to the  $-\text{C}-\text{N}-\text{C}-$  group of diethylenetriamine.<sup>19</sup> The elemental analysis data and functional group density of N in Table II also show that the amounts of nitrogen in CTSN-beads increase comparing with those in CTS and CTS-beads. These results indicate that the introduction of diethylenetriamine and the increasing of amine groups were achieved by chemical modification.

#### Effect of pH and Sorption Mechanism

The pH of the dye solution plays an important role in the adsorption process and particularly in the adsorption capacity, influencing not only surface charge of adsorbent and the electrostatic interaction between adsorbent and dyestuff, but also the solubility of beads and dyes. In this work, the modified CTS-beads are insoluble in 2% HCl, while the unmodified chitosan dissolves in acidic solutions below pH 5.5. The influence of pH on the adsorption capacity of dyes onto the CTSN-beads was observed over a pH range of 3–12 as illustrated in Figure 4. It can be seen that the sorption capacities decrease slowly from pH 3 to 9 and decreases dramatically in the pH range of 10–12. This result may be attributed to the electrostatic interaction between the protonated amine groups and the target dyes. In acidic medium, positive surface charge is developed owing to protonation of CTSN-beads which increases with the increase in  $\text{H}^+$  (decrease in pH). The progress of the adsorption is shown in Figure 5. In basic medium, base abstracts the  $\text{H}^+$  of amine groups and makes the surface of CTSN-beads negative. The appearance of electrostatic repulsion leads to decrease of sorption ability. It is reported<sup>16</sup> that the appropriate range of pH for applying unmodified chitosan is 5–7, whereas the wide applied range of pH (3–9) could be advantageous to the use of CTSN-beads as an adsorbent in removing dyes.

#### Effect of Contact Time and Sorption Kinetics

Figure 6 shows the effect of contact time on the adsorption capacity of the CTSN-beads with respect to the anionic dyes. The adsorption processes were divided into two stages. The first is a fast increase stage which lasts for 800 min and most dyes are removed. The second one is a slower stage standing for 48 h to reach equilibrium. In order to investigate the mechanism and rate-limiting step of adsorption, the second-order adsorption

models<sup>24,25</sup> were employed to deal with the kinetic data. The second-order model nonlinear form can be written as follow:

$$\text{Pseudo-second-order: } q_t = \frac{k_2 q_e^2 t}{1 + k_2 q_e t} \quad (2)$$

where  $k_2$  is the rate constant of second-order adsorption models ( $\text{g mmol}^{-1} \text{min}^{-1}$ ) respectively,  $q_e$  and  $q_t$  are the amount of dye absorbed at equilibrium and time  $t$  (min), both in  $\text{mmol g}^{-1}$ . And the initial sorption rate  $h$  ( $\text{mmol g}^{-1} \text{min}^{-1}$ ) can be calculated as follows:

$$h = k_2 q_e^2 \quad (3)$$

The parameters of kinetic models obtained by linearization procedure followed by linear regression analysis are shown in Table III. The pseudo-second-order predicted  $q_e$  of all dyes agree with the experimental data very well. These results suggest that the pseudo-second-order adsorption mechanism is applicable, and chemisorption might be the rate-limited step.<sup>26,27</sup> The initial sorption rate  $h$  and the rate constant of pseudo-second-order adsorption model for each dye follow the sequence

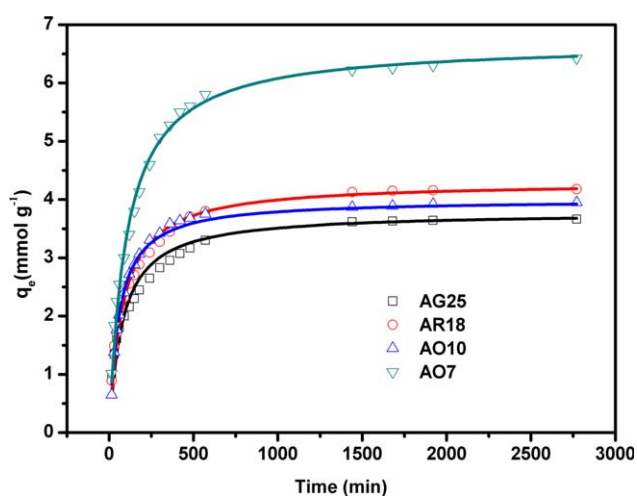


Figure 6. Effect of contact time on acid dyes adsorption on to CTSN-beads (the real lines represent modeled results using the pseudo-second-order equation). [Color figure can be viewed in the online issue, which is available at [wileyonlinelibrary.com](http://wileyonlinelibrary.com).]

**Table III.** Parameters of Pseudo-Second-Order Model and Freundlich Isotherm for Acid Dyes Adsorption onto CTSN-Beads

Dye	Pseudo-second-order				Freundlich isotherm		
	$k_2$ (g mmol <sup>-1</sup> min <sup>-1</sup> )	$q_e$ (mmol g <sup>-1</sup> )	$h$ (mmol g <sup>-1</sup> min <sup>-1</sup> )	$R^2$	$K_F$ (mmol <sup>1-1/n</sup> L <sup>1/n</sup> g <sup>-1</sup> )	$1/n$	$R^2$
AG25	0.0034	3.7810	0.0491	0.9589	4.0768	0.1385	0.9230
AR18	0.0032	4.2384	0.0577	0.9863	4.4284	0.1025	0.9359
AO10	0.0042	4.0532	0.0689	0.9940	3.8950	0.0648	0.9506
AO7	0.0015	6.6914	0.0662	0.9914	6.4061	0.0916	0.9038

AO10 > AO7 > AR18 > AG25. Obviously, the adsorption rate was directly related to both the molecular size of the dye and the amount of the sulfonate groups. Similar results were reported by Cestari et al.<sup>28</sup> and Maghami et al.<sup>29</sup> After modification, the pores in the net structure of beads can help the mass transfer of dyes, especially for the smaller molecular size dyes. So the adsorption rates and initial sorption rate of smaller dyes (AO7 and AO10) are much higher than those bigger dyes (AG25 and AR18). The molecular size of AO10 is close to that of AO7; however the adsorption rate of AO10 is higher than that of AO7, which is attributed to the amounts of sulfonate groups. For AO7, its molecular size is smaller than that of AR18, accelerating fast adsorption of dyes. AR18 has more sulfonate groups and smaller in size than those of AG25, the strong synergism effect enhanced the adsorption rate of AR18. For AO10, the smaller molecular size not only increases the concentration of dye on the surface of adsorbent but also gives an advantage to spread into the internal structure of CTSN-beads fleetly. And the respectable amounts of sulfonate groups enhance the electrostatic interaction between CTSN-beads and dyes to increase the adsorption rate.

#### Adsorption Equilibrium

The adsorption isotherm is fundamental to understand how pollutants interact with adsorbents. For optimizing the system of removing dyes, two isotherms (Freundlich and Langmuir–Freundlich isotherms) were applied to deal with the experimental data. The Freundlich model expresses the adsorption on the heterogeneous surfaces with interaction between adsorbed molecules.<sup>30,31</sup> It is an empirical approach applicable to the adsorption of high and medium concentration range, and it can be written as follows:

$$q_e = K_F C_e^{1/n} \quad (4)$$

where  $K_F$  and  $1/n$  are Freundlich constants that indicate the extent of sorption (mmol<sup>1-1/n</sup> L<sup>1/n</sup> g<sup>-1</sup>) and the sorption effectiveness. Meanwhile, the Langmuir–Freundlich isotherm, generalized for mixed-gas adsorption on solid, is probably the most frequently applied equation in technological applications.<sup>32</sup> This isotherm based on the generalized Langmuir and Freundlich isotherms is expressed as

$$q_e = \frac{q_m (K_{FL} C_e)^v}{1 + (K_{FL} C_e)^v} \quad (5)$$

where  $K_{FL}$  is the Langmuir–Freundlich constant L<sup>1/v</sup> mmol<sup>1-1/v</sup> and  $q_m$  is the maximum adsorption (mmol g<sup>-1</sup>),  $v$  is the Langmuir–Freundlich heterogeneous constant.

The parameters of Freundlich isotherm are listed in Table III. The Freundlich isotherm was found to provide a better theoretic

cal correlation of the experimental data for the sorption, which suggests that the adsorption behavior of CTSN-beads are more complicated than that of raw chitosan, and the adsorbed layer is more than one molecule thick. However, The Freundlich isotherm cannot provide satisfactory fits for AO7, so the Langmuir–Freundlich model was applied. The adsorptions based on this model are shown in Figure 7, and the parameters are listed in Table IV. This result shows that the Langmuir–Freundlich isotherm is represented. The capacity of CTSN-beads for each dye follows the sequence AO7 > AR18 > AO10 > AG25. The difference in the degree of adsorption may be attributed to the size and the chemical structure of the dye molecules.<sup>33</sup> The smaller size of AO7 not only increases the concentration of dye on the surface of beads, but also overcomes the interior steric hindrance of adsorbents having more active sites. On the contrary, the AG25 and AR18 due to bigger size were hindered the deeper penetration into the internal pore structure of adsorbent induced to the decrease of adsorption capacity. A similar interpretation was also previously given by Wong et al.<sup>34</sup> However, AO10 with the similar molecular size to AO7 represents lower  $q_m$ . There are two explanations for it. First, AO10 contains two sulfonate groups which may occupy more protonated amine groups, and thus reduce the adsorption capacity. Secondly, the anionic dyes with sulfonate groups on benzene can be more easily adsorbed than that of sulfonate groups on naphthalene. The similar behavior was also mentioned by Tsai et al.<sup>35</sup> Compared

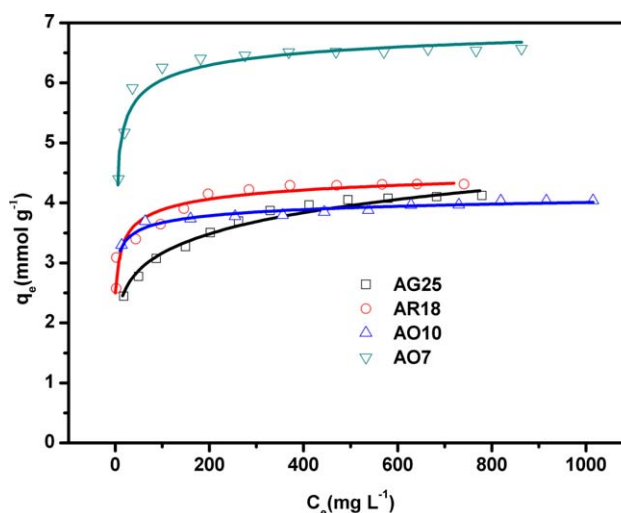


**Figure 7.** Adsorption isotherms fitted to Langmuir–Freundlich equation (the real lines). [Color figure can be viewed in the online issue, which is available at [wileyonlinelibrary.com](http://wileyonlinelibrary.com).]

**Table IV.** Parameters of Langmuir-Freundlich Isotherms for Acid Dyes Adsorption onto CTSN-Beads

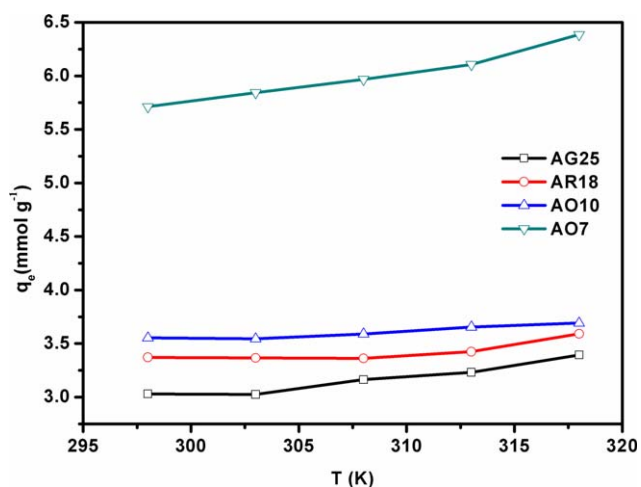
Dye	$q_m$ (mmol g <sup>-1</sup> )	$K_{LF}$ (L <sup>1/n</sup> mmol <sup>1-1/n</sup> )	$V$	$R^2$
AG25	4.2093	120.5	0.3490	0.9886
AR18	4.9419	322.0	0.3272	0.9600
AO10	4.5427	1421.9	0.2494	0.9903
AO7	7.2857	243.4	0.3748	0.9812

with some data in the literature, Table V shows that the CTSN-beads studied in this work have great adsorption capacity. For instance, the  $q_m$  for AO7 can reach 7.29 mmol g<sup>-1</sup> (4.54 mmol g<sup>-1</sup> for CTS and 6.32 mmol g<sup>-1</sup> for CTS-beads), but there are only 3.75 mmol of active amine groups contained in 1 g of raw chitosan (91.2% of deacetylation degree). Obviously, this indicated that pretreating and grafting can not only increase the amounts and utilization rate of active amine groups efficiently but also reduce the steric hindrance during the sorption process.

#### Effect of Adsorption Temperature

It is well known that temperature plays an important role in adsorption. The results of the effect of adsorption temperature (ranged from 293 to 318 K) are shown in Figure 8. Generally speaking, high temperature has a negative influence on the amount of dyes adsorbed. However, it can be obtained from Figure 8 that an increase in temperature leads to a raise in the amount of adsorbed dye at equilibrium. The high temperature increased the dimension of the chitosan pores, and thus increased the adsorption capacities. Cestari et al.<sup>28</sup> and Uzun and Güzel<sup>36</sup> also found similar phenomenon, suggesting that adsorption study in this work is endothermic and it has been proved by the following expression.

To further verify the result, the thermodynamic parameters of the adsorption were determined by applying Van't Hoff equation and Gibbs expression:

**Figure 8.** Effect of temperature on acid dyes adsorption by CTSN-beads. [Color figure can be viewed in the online issue, which is available at [wileyonlinelibrary.com](http://wileyonlinelibrary.com).]

$$\ln K_L = \frac{\Delta H^\theta}{RT} + \frac{\Delta S^\theta}{R} \quad (6)$$

$$K_L = \frac{q_e}{C_e} \quad (7)$$

$$\Delta G^\theta = -RT \ln K_L = \Delta H^\theta - T\Delta S^\theta \quad (8)$$

where  $R$  is the universal gas constant (8.314 J mol<sup>-1</sup> K<sup>-1</sup>), the calculated  $\Delta H^\theta$  (enthalpy change),  $\Delta S^\theta$  (entropy change), and  $\Delta G^\theta$  (Gibbs free energy change) are reported in Table VI. The positive values of  $\Delta H^\theta$  implies that the adsorption phenomenon is endothermic. Moreover, the negative value of  $\Delta S^\theta$  and  $\Delta G^\theta$  indicate that the adsorption processes will occur spontaneously.  $\Delta G^\theta$  was more negative with increasing temperature, which suggested that higher temperature makes the adsorption easier.

#### Desorption and Reuse

The regeneration of the loaded adsorbents was essential as the adsorbent can be recycled for dyeing wool. The sodium sulfate in the adsorption solution can screen the coulombic potential between the dyes and charged adsorbents. The adsorption

**Table V.** Comparison of Maximum Adsorption Capacities of Dyes on Various Adsorbents

Reference	Dyes adsorption capacities (mmol g <sup>-1</sup> )				Adsorbent
	AO7	AO10	AG25	AR18	
This work	7.29	4.54	4.21	4.94	Diethylenetriamine-modified CTS-bead
36	0.83	0.44	0.31	0.38	Dithiocarbamate-modified starch
37	2.52	1.24	1.80	1.57	Diethylenetriamine-modified enzymatic hydrolysis starch
38		0.53	0.87		Ethylenediamine modified starch
16	5.54				CTS-bead(cross-linked,TPP)
39		1.5	1.05	1.2	Chitosan
32	3.47	2.25			Ethylenediamine-modified magnetic chitosan nanoparticles
40		1.77		1.37	Chitosan nanoparticles
35			1.36		Chitosan

**Table VI.** Thermodynamic Values at Various Temperatures for the Dyes Adsorbed onto CTSN-Beads

Dye	$\Delta H^\theta$ (kJ mol <sup>-1</sup> )	$\Delta S^\theta$ (J mol <sup>-1</sup> K <sup>-1</sup> )	$\Delta G^\theta$ (kJ mol <sup>-1</sup> )				
			298 K	303 K	308 K	313 K	318 K
AG25	20.81	-87.98	-5.57	-5.69	-6.20	-6.68	-7.29
AR18	22.49	-96.23	-6.36	-6.59	-6.92	-7.54	-8.31
AO10	5.15	-31.43	-4.27	-4.31	-4.50	-4.73	-4.85
AO7	23.37	-98.93	-6.16	-6.60	-7.07	-7.45	-8.21

**Table VII.** Comparison of Maximum Adsorption Capacities of Dyes on Fresh and Regeneration CTSN-Beads

Dye	$q_e$ (mmol g <sup>-1</sup> )	
	Fresh	After 5 cleaning cycle
AO7	6.32	5.91
AO10	3.81	3.56
AG25	3.36	2.86
AR18	3.74	3.41

capacity decreases dramatically when the concentration of sodium sulfate is over 0.01 mmol L<sup>-1</sup>. The positively charged amino groups were deprotonated and the electrostatic interaction between adsorbents and dye molecules became weaker in the basic environment. So the Na<sub>2</sub>SO<sub>4</sub>/NaOH (pH 12.0) solution was chosen to regenerate the CTSN-beads. The desorption agent can remove about 85–90% absorbed dyes. The maximum adsorption capacities of dyes on fresh and regeneration CTSN-beads after five cleaning cycle are shown in Table VII. It was observed that adsorption capacities of the regeneration CTSN-beads for dyes (except AG25) still retained 90% capacities as those of the fresh adsorbents. The lower regeneration capacities for AG25 loaded CTSN-beads could be attributed to the hydrogen bonds between AG25 and adsorbents. The hydrogen bonds formed by carbonyl groups of AG25<sup>38</sup> were much stronger than the electrostatic interaction. The results indicated that the CTSN-beads can be recovered for multiple uses.

## CONCLUSION

In summary, the chitosan beads were modified with diethylenetriamine to obtain an excellent adsorbent, the CTSN-beads. A batch system was applied to study the adsorption properties of CTSN-beads for four acid dyes: Acid orange 7 (AO7), Acid orange 10 (AO10), Acid red 18 (AR18), and Acid green 25 (AG25), from aqueous solutions. The adsorption capacities for dyes are 2–10 times as much as those of the chitosan and chitosan derivatives reported. The IR analysis result proves the successful synthesis of CTSN-beads. The research also showed that the adsorption mechanism was based on electrostatic interaction. The equilibrium data fitted well with Langmuir–Freundlich isotherm. The adsorption rate and capacities were directly related to the molecular size of the dye and the amount of the sulfonate groups on the dye molecules. The positive enthalpy energy change for the adsorption process confirms the exothermic nature of adsorption, and a free energy change confirms the spontaneity of the process. Although

considerable information has been collected for the adsorption of single component dyes by CTSN-beads, many industrial situations involve the discharge of effluents that contain a mixture of several dyes. The study of multi-component adsorption should be present for future research.

## ACKNOWLEDGMENTS

This work was supported by Experimental Chemistry Center Tongji University, Shanghai. The authors thank Dr. Zuohua Wang for assistance during this work.

## REFERENCES

- Robinson, T.; McMullan, G.; Marchant, R.; Nigam, P. *Biore-sour. Technol.* **2001**, *77*, 247.
- Muthukumar, M.; Sargunamani, D.; Selvakumar, N. *Dyes Pigm.* **2005**, *65*, 151.
- Körbahti, B. K.; Tanyolaç, A. *J. Hazard. Mater.* **2009**, *170*, 771.
- Hai, F. I.; Yamamoto, K.; Nakajima, F.; Fukushi, K. *J. Membr. Sci.* **2008**, *325*, 395.
- Al-Degs, Y. S.; El-Barghouthi, M. I.; El-Sheikh, A. H.; Walker, G. M. *Dyes Pigm.* **2008**, *77*, 16.
- Kim, T.; Son, Y.; Lim, Y. *Dyes Pigm.* **2005**, *64*, 73.
- Su, Y.; Zhang, Y.; Wang, J.; Zhou, J.; Lu, X.; Lu, H. *Biore-sour. Technol.* **2009**, *100*, 2982.
- Silva, A. C.; Pic, J. S.; Sant Anna, G. L., Jr.; Dezotti, M. *J. Hazard. Mater.* **2009**, *169*, 965.
- Szygula, A.; Guibal, E.; Ruiz, M.; Sastre, A. M. *Colloids Surf. A* **2008**, *330*, 219.
- Xu, S.; Wang, J.; Wu, R.; Wang, J.; Li, H. *Chem. Eng. J.* **2006**, *117*, 161.
- Iqbal, M.; Saeed, A. *Process. Biochem.* **2007**, *42*, 1160.
- Dolphen, R.; Sakkayawong, N.; Thiravetyan, P.; Nakbanpote, W. *J. Hazard. Mater.* **2007**, *145*, 250.
- Stephen Inbaraj, B.; Chen, B. H. *Biore-sour. Technol.* **2011**, *102*, 8868.
- Szygula, A.; Guibal, E.; Palacín, M. A.; Ruiz, M.; Sastre, A. M. *J. Environ. Manage.* **2009**, *90*, 2979.
- Kyzas, G. Z.; Lazaridis, N. K. *J. Colloid Interface Sci.* **2009**, *331*, 32.
- Chiou, M.; Ho, P.; Li, H. *Dyes Pigm.* **2004**, *60*, 69.
- Chatterjee, S.; Chatterjee, S.; Chatterjee, B. P.; Das, A. R.; Guha, A. K. *J. Colloid Interface Sci.* **2005**, *288*, 30.



18. Guibal, E.; Milot, C.; Eterradossi, O.; Gauffier, C.; Domard, A. *Int. J. Biol. Macromol.* **1999**, *24*, 49.
19. Yi, Y.; Wang, Y.; Ye, F. *Colloids Surf. A* **2006**, *277*, 69.
20. Wang, Z.; Bo, X.; Zheng, Z.; Li, Y. *Adv. Mater. Res.* (Durnten-Zurich, Switzerland). **2011**, 236–238, 464.
21. Jeon, C.; Höll, W. H. *Water Res.* **2003**, *37*, 4770.
22. Li, N.; Bai, R. *Ind. Eng. Chem. Res.* **2005**, *44*, 6692.
23. Rajiv Gandhi, M.; Kousalya, G. N.; Viswanathan, N.; Meenakshi, S. *Carbohydr. Polym.* **2011**, *83*, 1082.
24. Cestari, A. R.; Vieira, E. F. S.; Dos Santos, A. G. P.; Mota, J. A.; de Almeida, V. P. *J. Colloid Interface Sci.* **2004**, *280*, 380.
25. Ho, Y. S.; McKay, G. *Process. Saf. Environ.* **1998**, *76*, 183.
26. Ho, Y. S.; McKay, G. *Process. Saf. Environ.* **1998**, *76*, 332.
27. Ho, Y. S.; McKay, G. *Process. Biochem.* **1999**, *34*, 451.
28. Cestari, A. R.; Vieira, E. F. S.; Pinto, A. A.; Lopes, E. C. N. *J. Colloid Interface Sci.* **2005**, *292*, 363.
29. Maghami, G. G.; Roberts, G. A. F. *Die Makromol. Chem.* **1988**, *189*, 2239.
30. Giles, C. H.; D'Silva, A. P.; Easton, I. A. *J. Colloid Interface Sci.* **1974**, *47*, 766.
31. Ngah, W. S. W.; Fatinathan, S. *J. Environ. Manage.* **2010**, *91*, 958.
32. Rudziński, W.; Dominko, A.; Wojciechowski, B. W. *Chem. Eng. J. Biochem. Eng. J.* **1996**, *64*, 85.
33. Zhou, L.; Jin, J.; Liu, Z.; Liang, X.; Shang, C. *J. Hazard. Mater.* **2011**, *185*, 1045.
34. Wong, Y. C.; Szeto, Y. S.; Cheung, W. H.; McKay, G. *Process. Biochem.* **2004**, *39*, 695.
35. Tsai, W. T.; Chang, C. Y.; Ing, C. H.; Chang, C. F. *J. Colloid Interface Sci.* **2004**, *275*, 72.
36. Uzun, İ.; Güzel, F. *J. Colloid Interface Sci.* **2004**, *274*, 398.
37. Cheng, R.; Xiang, B.; Li, Y.; Zhang, M. *J. Hazard. Mater.* **2011**, *188*, 254.
38. Wang, Z.; Xiang, B.; Cheng, R.; Li, Y. *J. Hazard. Mater.* **2010**, *183*, 224.
39. Cheng, R.; Ou, S.; Li, M.; Li, Y.; Xiang, B. *J. Hazard. Mater.* **2009**, *172*, 1665.
40. Wong, Y. C.; Szeto, Y. S.; Cheung, W. H.; McKay, G. *Langmuir* **2003**, *19*, 7888.